J. Fluid Mech. (1970), *vol.* 42, *part* 3, *pp.* 513–525
Printed in Great Britain

The development of horizontal boundary layers in stratified flow. Part 2. Diffusive flow

By L. G. REDEKOPP

Department of Aerospace Engineering
University of Colorado
Boulder, Colorado 80302

(Received 15 September 1969)

The boundary layer on the upper surface of a horizontal plane in a diffusive, stratified flow is examined. The analysis shows that density diffusion increases the role of the buoyancy forces and causes a significant change in the properties of the boundary layer when compared to the non-diffusive case. A uniformly valid first approximation for moderate Russell numbers is derived, and the effects of buoyancy and diffusion are evaluated by solving the resulting equations numerically.

1. Introduction

In part 1 of this series (Kelly & Redekopp 1970, hereafter referred to as I), we examined the boundary-layer structure for steady, stratified fluid motions on the assumption that the Prandtl (or Schmidt) number was very large, whereby the effects of density diffusion could be neglected. The results showed that three different régimes of flow are possible, depending on the relative magnitudes of the Reynolds and Russell numbers, and demonstrated that the coupling between the boundary layer and the external flow plays a crucial role in determining the overall features of the flow.

Martin & Long (1968) considered the effect of diffusion for the flow over a flat plate when the velocity boundary layer grows in the upstream direction. They show that the diffusion boundary layer grows from the leading edge irrespective of the Russell number. Obviously then, the diffusion and velocity layers intersect somewhere over the plate surface, and diffusion can strongly affect the trailing-edge singularity and the existence of a downstream wake. The analysis of Martin & Long (1968), however, was limited to large Schmidt (Prandtl) numbers and to the flow region near the leading edge of the plate where the velocity boundary layer is thick relative to the diffusion boundary layer.

In the present paper, the restriction to large Prandtl numbers imposed in I is relaxed in order to establish the effect of density diffusion on the flow structure in general and the boundary-layer properties in particular. It is known that the relative thickness of the viscous and diffusion boundary layers is determined solely by the magnitude of the Prandtl number. Hence, when the Prandtl number is of order unity or smaller, the coupling between the velocity and thermal fields can be expected to be important, especially within the boundary layer. Also,

heat diffusion can contribute significantly to the magnitude of buoyancy forces in the boundary layer and furthermore, as the Prandtl number decreases, the vertical scale over which these buoyancy forces act is increased. The combination of these effects is investigated for the flow over a horizontal plane. The general flow structure above a finite plate with diffusion is discussed in § 3 and a similarity solution of the boundary-layer equations with buoyancy and heat diffusion is derived in § 4. Numerical results are presented in § 5.

2. Formulation

We consider the development of the velocity and thermal boundary layers on the upper surface of an isothermal, horizontal plate of length L immersed in a fluid that is in uniform motion with velocity U_0. The fluid is assumed to be stably stratified, and the stratification is assumed to derive from a linear space-distribution of temperature given by

$$T_{s(x_3)} = T_0(1+\beta_0 x_3). \tag{1}$$

A schematic of the flow configuration is given in figure 1. The fluid motion is assumed to obey the Boussinesq equations, which for the steady flow of a viscous, heat-conducting fluid are

$$\nabla . \mathbf{q} = 0, \tag{2}$$

$$(\mathbf{q}.\nabla)\mathbf{q} = -\frac{1}{\rho_0}\nabla p - \frac{\rho}{\rho_0} g\hat{\mathbf{k}} + \nu_0 \nabla^2 \mathbf{q}, \tag{3}$$

$$(\mathbf{q}.\nabla)T = \kappa_0 \nabla^2 T \tag{4}$$

and

$$\rho = \rho_0[1-\alpha_0(T-T_0)]. \tag{5}$$

The quantities $\mathbf{q}, p, \rho$, and T are, respectively, the velocity, pressure, density, and temperature of the fluid at the point (x_1, x_3); ν_0 and κ_0 denote the kinematic viscosity and thermal diffusivity (which are constants in the limit of the Boussinesq approximation; α_0 represents the coefficient of thermal expansion; and $\hat{\mathbf{k}}$ is a unit vector in the vertical direction. Symbols with the subscript '0' correspond to undisturbed values at the altitude of the plate ($x_3 = 0$). Use of the linear density-temperature relation (5) and a linear stratification in an unbounded flow is consistent with the Boussinesq approximation providing $(\alpha_0 T_0 \beta_0)^{-1}$ is large compared to a characteristic vertical dimension of the phenomena being described (e.g. the boundary-layer thickness).

Introducing the dimensionless state variables

$$T^* = \frac{T_{(x_1,x_3)}-T_0}{T_w-T_0} - \frac{T_0\beta_0 x_3}{T_w-T_0} = \frac{T-T_0}{T_w-T_0} - \frac{\beta}{\theta} z, \tag{6}$$

$$\rho^* = \frac{\rho}{\rho_0} = 1-\alpha(\beta z + \theta T^*) \tag{7}$$

and

$$p^* = \frac{p-p_0}{\rho_0 U_0^2} + \frac{1}{F_L}[z - \tfrac{1}{2}\alpha\beta z^2], \tag{8}$$

and following a procedure similar to that used in I, the system of equations (2) to (4) can be reduced to the set of coupled equations

$$\left[L(x,z,\psi)-\frac{1}{R_L}\nabla^2\right]\nabla^2\psi+\frac{\alpha\theta}{F_L}T_x=0, \tag{9}$$

and

$$\left[L(x,z,\psi)-\frac{1}{P_0R_L}\nabla^2\right](z\beta/\theta+T)=0. \tag{10}$$

The stream function ψ, Froude number F_L, Prandtl number P_0, Reynolds number R_L, and operator $L(x,z,\psi)$ are defined in I, θ represents the thermal driving potential across the boundary layer

$$\theta=\frac{T_w-T_0}{T_0}, \tag{11}$$

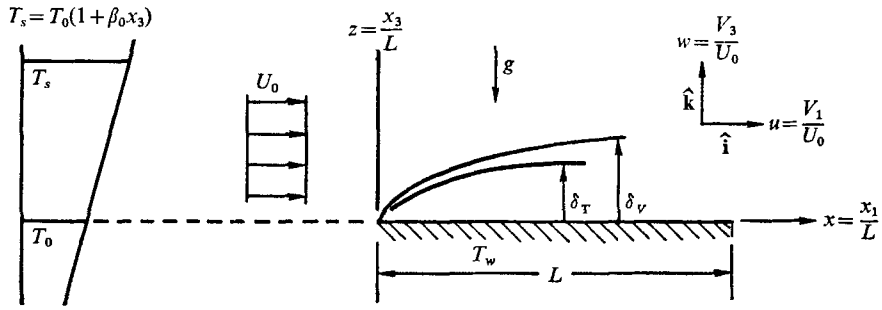

FIGURE 1. A schematic of the flow model.

β is a dimensionless stratification scale ($\beta_0 L$), and α denotes a dimensionless thermal expansion coefficient ($\alpha_0 T_0$). The asterisk has been deleted from the temperature since all the variables are clearly dimensionless. In what follows, α will be taken to be unity, which is the case for a perfect gas, and the ratio β/θ is taken to be of order unity. The results can be applied to any fluid with arbitrary α by multiplying θ and β by α as can be seen from (9) and (10). Both ($\alpha\theta$) and ($\alpha\beta$) must be smaller than unity for the Boussinesq approximation to be valid. The limiting case of θ approaching zero requires that a new dimensionless temperature (θT^*) be defined, but then the boundary conditions will depend on θ.

In I we were able to combine the three parameters θ, β, and F_L into one parameter, the Russell number. That is possible only in the limit of infinite Prandtl number whereby the temperature is constant along a streamline. When the Prandtl number is finite, heat diffuses across streamlines and the simplified representation for T is destroyed. In the diffusive case, then, four basic parameters are required to describe the flow, and the characterization of the flow in a two-dimensional space (R_L, Ru_L) as in I is no longer possible.

The boundary conditions for the flow depicted in figure 1 are

$$\psi(x,0)=0, \tag{12a}$$

$$\psi_z(x,z\to\infty)=\psi_z(x\to-\infty,z)=1, \tag{12b}$$

$$T(x,z\to\infty)=T(x\to-\infty,z)=0, \tag{12c}$$

$$\psi_z(x,0)=0 \quad \text{for} \quad 0\leqslant x\leqslant 1 \tag{12d}$$

and

$$T(x,0)=1 \quad \text{for} \quad 0\leqslant x\leqslant 1. \tag{12e}$$

These conditions complete the specification of the problem under consideration.

Now we seek to obtain an approximate solution to equations (9) and (10) subject to (12) for the case when the Reynolds number is large compared to unity. The objective is to establish the effect stratification has on the velocity and temperature field near a horizontal boundary and also on the friction and heat transfer at the boundary.

3. The flow structure for arbitrary Russell number

The approximate solution of (9) and (10) for infinite Reynolds number satisfying the far-field conditions (12a, b, c) is

$$\psi = z \quad \text{and} \quad T = 0. \tag{13}$$

This solution fails near the plate surface due to the neglect of diffusion effects. In the immediate vicinity of the plate the diffusion of vorticity and heat are essential to a description of the flow. We emphasize this explicitly by expanding the vertical scale in the manner

$$y = z/\epsilon(R_L), \tag{14}$$

where $\epsilon(R_L)$ scales the thickness of the viscous boundary layer and tends to zero in the limit as R_L tends to infinity. Another scale $\epsilon_T(P_0, R_L)$ characteristic of the thermal-diffusion boundary-layer thickness can be defined, but, at least for the Blasius boundary layer, it is directly related to $\epsilon(R_L)$ by the expression

$$\frac{\epsilon}{\epsilon_T} = P_0^{\frac{1}{2}} = \frac{\delta_v}{\delta_T}. \tag{15}$$

This relation portrays clearly the role of the Prandtl number. In subsequent sections we take the Prandtl number to be of order unity whereby the distinction between the two scales is irrelevant.

Substituting (14) into (9) and (10) yields the boundary-layer vorticity and energy equations in the forms

$$\left[L(x,y,\Psi) - \frac{\epsilon^{-2}}{R_L}\left(\epsilon^2\frac{\partial^2}{\partial x^2} + \frac{\partial^2}{\partial y^2}\right)\right]\left(\epsilon^2\frac{\partial^2}{\partial x^2} + \frac{\partial^2}{\partial y^2}\right)\Psi + \epsilon(\theta/\beta)\,Ru_L^2\,\tilde{T}_x = 0, \tag{16}$$

and

$$\left[L(x,y,\Psi) - \frac{\epsilon^{-2}}{P_0 R_L}\left(\epsilon^2\frac{\partial^2}{\partial x^2} + \frac{\partial^2}{\partial y^2}\right)\right]\tilde{T} - \epsilon(\beta/\theta)\Psi_x = 0. \tag{17}$$

The new dependent variables are defined by

$$\psi(x,z) = \epsilon(R_L)\Psi(x,y) = \epsilon[\Psi^{(1)}(x,y) + \alpha(R_L)\Psi^{(2)}(x,y) + \ldots] \tag{18a}$$

and

$$T(x,z) = \tilde{T}(x,y) = \tilde{T}^{(1)}(x,y) + \Delta(R_L)\tilde{T}^{(2)}(x,y) + \ldots, \tag{18b}$$

and the Russell number β/F_L has been introduced for comparison with the results of I. The transformations (18) arise from the matching requirements between the boundary layer and external stream (13). Using the parameter representation

$$Ru_L^2 = R_L^n \tag{19}$$

as in I, we see that the inertia-viscous (Blasius) boundary-layer balance with the familiar scale $\epsilon = R_L^{-\frac{1}{2}}$ holds for $n < \frac{1}{2}$, in contrast with $n = 1$ in the non-diffusive

case. Diffusion increases the role of buoyancy forces within the boundary layer and thereby can significantly alter the structure of the flow field. Recalling that β/θ is of order one, the direct effect of stratification (the last term in (17)) is at most a second-order quantity, and the scale of the diffusion boundary layer ($\epsilon_T = (P_0 R_L)^{-\frac{1}{2}}$) is unaffected by the stratification.

The region of applicability of the non-diffusive approximation is now clear. It requires that the Prandtl number be larger than $\epsilon^{-1} = R_L^{\frac{1}{2}}$ for the first-order boundary-layer analysis when $n < \frac{1}{2}$. For $n > \frac{1}{2}$, the buoyancy and viscous terms in (16) must balance leading to the scale

$$\epsilon = \epsilon_{bv} = (R_L R u_L^2)^{-\frac{1}{3}} = R_L^{-\frac{1}{3}(1+n)}, \tag{20}$$

and the first-order vorticity equation becomes

$$\Psi^{(1)}_{yyyy} - \tilde{T}^{(1)}_x = 0. \tag{21}$$

The energy equation (17) for the corrresponding scale is

$$\left[P_0 L(z, y, \Psi) - R_L^{\frac{1}{3}(2n-1)} \left(\epsilon_{bv}^2 \frac{\partial^2}{\partial x^2} + \frac{\partial^2}{\partial y^2}\right)\right] \tilde{T} - P_0 \epsilon_{bv} (\beta/\theta) \Psi_x = 0. \tag{22}$$

which shows that, for Prandtl numbers satisfying the condition

$$P_0 = R_L^{\frac{1}{3}(2n-1)} \quad (n > \tfrac{1}{2}), \tag{23}$$

the first-order equation is a balance between convection and diffusion. However, for Prandtl numbers smaller than that given in (23), the flow is diffusive on this scale. For Prandtl numbers greater than the condition (23), the first-order energy equation is non-diffusive on the scale of (20), but a diffusion layer does exist with a scale smaller than (20). Similarly, one can show that when the Prandtl number is larger than $R_L^{\frac{1}{2}(3n-1)}$, $n > 1$, the boundary-layer flow correct to first-order is described by the non-diffusive solution of Martin & Long (1968) and, when the Prandtl number is smaller than R_L^{-1}, the entire flow is diffusive ($\epsilon_T = O(1)$). A unified view of these results is given in figure 2 where n is defined by (19) and m is defined by the relation

$$P_0 = R_L^m. \tag{24}$$

The first-order flow characteristics are indicated in the respective domains on the figure.

In the outer flow where diffusion effects are negligible (at least to second order), (9) and (10) yield

$$L(x, z, \psi) \nabla^2 \psi + R u_L^2 \psi_x = 0, \tag{25a}$$

and

$$T = (\beta/\theta)(\psi - z). \tag{25b}$$

These equations are identical to the outer flow equations in I and, therefore, exhibit the same characteristics depending on the magnitude of the Russell number. However, since the first-order boundary layer is the Blasius one for all $n < \frac{1}{2}$, another scaling of the equations (9) and (10) is required for the parameter range $0 < n < \frac{1}{2}$ as compared to the range $0 < n < 1$ for the non-diffusive case. The correct intermediate-layer scaling for the diffusive case is the same as in I, namely,

$$(\hat{x}, \hat{y}) = (x, y) R_L^{\frac{1}{2}n} \quad (0 \leqslant n < \tfrac{1}{2}). \tag{26}$$

The matching conditions require that the expansions for the dependent variables in the intermediate layer have the form

$$\psi(x,z) = R_L^{-\frac{1}{2}n}\hat{\Psi}(\hat{x},\hat{y}) = R_L^{-\frac{1}{2}n}[\hat{y} + R_L^{-\frac{1}{2}(1-\frac{1}{2}n)}\hat{\Psi}^{(1)}(\hat{x},\hat{y}) + \ldots], \tag{27a}$$

and

$$T(x,z) = R_L^{-\frac{1}{2}(1+\frac{1}{2}n)}\hat{T}^{(1)}(\hat{x},\hat{y}) + \ldots \quad (0 \leqslant n < \tfrac{1}{2}). \tag{27b}$$

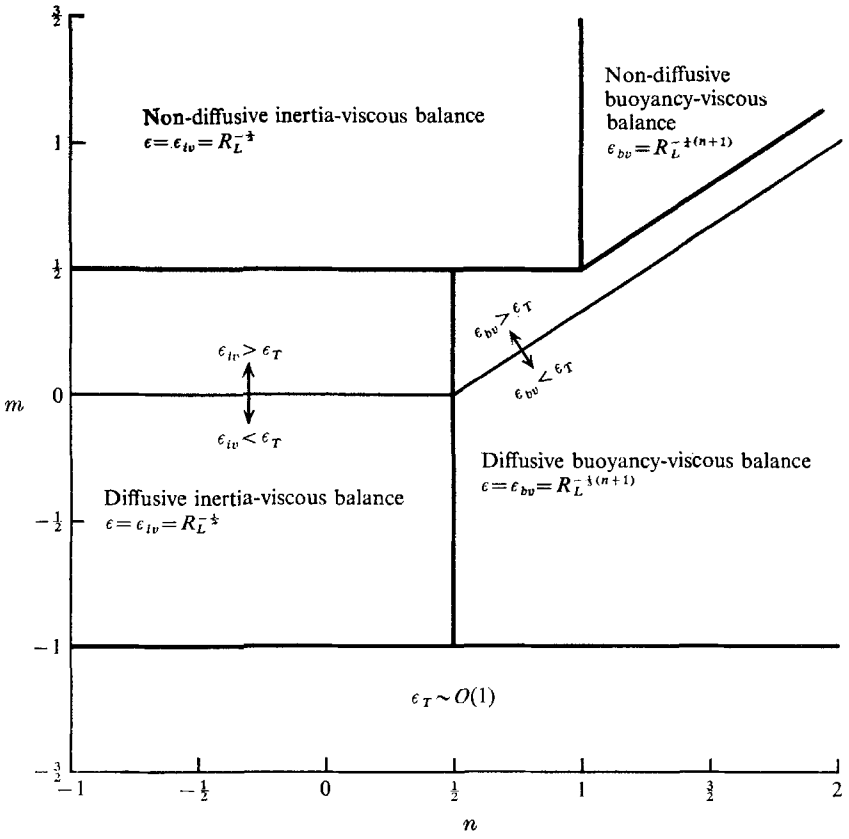

FIGURE 2. A unified representation of the first-order flow characteristics in Prandtl number–Russell number space.

The function $\hat{\Psi}^{(1)}$ is determined from the solution of the Helmholtz equation as in I (§6) and

$$\hat{T}^{(1)}(\hat{x},\hat{y}) = (\beta/\theta)\hat{\Psi}^{(1)}(\hat{x},\hat{y}). \tag{28}$$

With these transformations, a uniformly valid first approximation to (9) and (10) is possible for all Russell numbers greater than or equal to zero. The condition $n = \frac{1}{2}$ is the critical stratification for the diffusive boundary layer and corresponds to a smaller stratification than the case $n = 1$ which is the critical condition for the non-diffusive boundary layer.

4. A similarity solution for the case $n = 0$

We now consider the particular case when the Russell number is of order unity ($n = 0$). Since the Reynolds number is presumed to be large, the parameter $\epsilon = R_L^{-\frac{1}{2}}$ is small, and it is reasonable to seek solutions of equations (16) and (17) by means of a perturbation analysis. The boundary-layer variables are expanded in a sequence of the form given by (18*a*, *b*). Similarly, the outer flow variables are expressed as

$$\psi(x,z) = z + \gamma(R_L)\psi^{(1)}(x,z) + \ldots, \tag{29a}$$

and

$$T(x,z) = 0 + \gamma(R_L)T^{(1)}(x,z) + \ldots, \tag{29b}$$

where the first terms on the right-hand side are known from (13). The functions $\gamma(R_L)$, $\alpha(R_L)$, $\Delta(R_L)$ are part of an asymptotic sequence and are determined by matching the two expansions (18) and (29). In this study we carry the expansion procedure only to the order indicated in (18) and (29).

Substituting (18) into (16) and (17) yields the first-order boundary-layer equations

$$\left[L(x,y,\Psi^{(1)}) - \frac{\partial^2}{\partial y^2}\right]\Psi^{(1)}_{yy} = 0 \tag{30a}$$

and

$$\left[L(x,y,\Psi^{(1)}) - \frac{1}{P_0}\frac{\partial^2}{\partial y^2}\right]\tilde{T}^{(1)} = 0. \tag{30b}$$

Introducing the variables

$$\eta = y/x^{\frac{1}{2}}, \Psi^{(1)}(x,y) = x^{\frac{1}{2}}f_1(\eta) \quad \text{and} \quad \tilde{T}^{(1)}(x,y) = h_1(\eta), \tag{31}$$

the above equations reduce to the familiar similarity forms

$$f_1''' + \tfrac{1}{2}f_1 f_1'' = 0 \tag{32a}$$

and

$$h_1'' + \tfrac{1}{2}P_0 f_1 h_1' = 0. \tag{32b}$$

The appropriate boundary conditions are

$$f_1(0) = f_1'(0) = h_1(\infty) = 0 \quad \text{and} \quad f_1'(\infty) = h_1(0) = 1. \tag{32c}$$

Note that the first-order problem depends only on one parameter, the Prandtl number. The solutions for f_1 and h_1 are known (cf. Schlichting 1968, pp. 126, 280). Using the properties of these solutions, we find the matching conditions

$$\gamma(R_L) = \epsilon = R_L^{-\frac{1}{2}} \quad \text{and} \quad \psi^{(1)}(x,0) = -1{\cdot}730x^{\frac{1}{2}} \quad (x > 0). \tag{33}$$

Consequently, $\psi^{(1)}$ is given by the solution of the Helmholtz equation (see I, §6) and $T^{(1)}$ obeys an equation analogous to (28).

Since the displacement thickness in the downstream wake is unknown, we assume that the outer flow can be calculated as if the plate were semi-infinite. The solution for $\psi^{(1)}$ (I, §6) shows that, for a semi-infinite plate, the induced horizontal velocity vanishes as z tends to zero. Within this approximation, there is no coupling between $\psi^{(1)}$ and $\Psi^{(2)}$ and the gauge function $\alpha(R_L)$ is undetermined. However, examining the relation for the temperature, we see that

$$T^{(1)}(x,0) = (\beta/\theta)\psi^{(1)}(x,0) = -1{\cdot}730(\beta/\theta)x^{\frac{1}{2}} \tag{34}$$

so that there is a coupling between the outer flow and the second-order boundary layer via the temperature field. The coupling is a direct consequence of the diffusion of heat. This requires that $\Delta(R_L) = \epsilon$ and, by substituting the respective expansions into the boundary-layer equations, one finds that $\alpha(R_L) = \epsilon$ as well.

By virtue of the above results, the second-order boundary-layer equations have the form

$$\left[L(x,y,\Psi^{(1)}) - \frac{\partial^2}{\partial y^2}\right]\Psi^{(2)}_{yy} + L(x,y,\Psi^{(2)})\,\Psi^{(1)}_{yy} + (\theta/\beta)\,Ru_L^2\,\tilde{T}^{(1)}_x = 0 \tag{35a}$$

and

$$\left[L(x,y,\Psi^{(1)}) - \frac{1}{P_0}\frac{\partial^2}{\partial y^2}\right]\tilde{T}^{(2)} + L(x,y,\Psi^{(2)})\,\tilde{T}^{(1)} - (\beta/\theta)\,\Psi^{(1)}_x = 0, \tag{35b}$$

with boundary conditions

$$\left.\begin{aligned} &\Psi^{(2)}(x,0) = \Psi^{(2)}_y(x,0) = \Psi^{(2)}_y(x,\infty) = \Psi^{(2)}_{yy}(x,\infty) = \tilde{T}^{(2)}(x,0) = 0 \\ \text{and}\quad &\tilde{T}^{(2)}(x,\infty) = -(\beta/\theta)1{\cdot}730x^{\frac{1}{2}}, \end{aligned}\right\} \tag{35c}$$

where the Russell number has been included to indicate explicitly its role, but its order of magnitude is assumed to be unity. Similarity forms are possible for these equations also if we write

$$\Psi^{(2)} = xf_2(\eta) \quad \text{and} \quad \tilde{T}^{(2)} = x^{\frac{1}{2}}h_2(\eta). \tag{36}$$

The equations for f_2 and h_2 are given by

$$2f'''_2 + f_1 f''_2 - f'_1 f'_2 + 2f''_1 f_2 = -(\theta/\beta)\,Ru_L^2\left[\eta h_1 + \int_\eta^\infty h_1\,d\eta\right], \tag{37a}$$

$$2h''_2 + P_0\{f_1 h'_2 - f'_1 h_2 + 2f_2 h'_1\} = P_0(\beta/\theta)\,(\eta f'_1 - f_1), \tag{37b}$$

subject to the conditions

$$f_2(0) = f'_2(0) = f'_2(\infty) = h_2(0) = 0 \quad \text{and} \quad h_2(\infty) = -(\beta/\theta)\,(1{\cdot}730). \tag{37c}$$

The first equation has been integrated once to reduce it to a third-order equation. The right-hand sides are known from the first-order solution (32) and comprise the primary forcing functions for the second-order boundary layer. A one-way coupling exists between (32) and (37) which proceeds from the first-order momentum equation (32a) to the second-order energy equation (37b). Furthermore, all equations except (32a) are linear. The combination of these facts simplifies considerably the numerical solution of the above equations.

Before discussing the numerical solutions to the above equations, it is worth pointing out that the boundary-layer expansion for the parameter range $0 < n < \frac{1}{2}$ has the form

$$\psi(x,z) = R_L^{-\frac{1}{2}}[\Psi^{(1)}(x,y) + R_L^{n-\frac{1}{2}}\Psi^{(2)}(x,y) + \ldots], \tag{38a}$$

and

$$T(x,z) = \tilde{T}^{(1)}(x,y) + R_L^{n-\frac{1}{2}}\tilde{T}^{(2)}(x,y) + \ldots. \tag{38b}$$

The equations for $\Psi^{(2)}$ and $\tilde{T}^{(2)}$ are identical to (35a, b) except that the term multiplied by the parameter β/θ in the energy equation (35b and 37b) does not appear. Thus, the solution of (37a) yields the second-order velocity field for the entire range $0 \leqslant n < \frac{1}{2}$. Furthermore, comparison of the expansions (27) and (38) shows that the second-order boundary-layer stream function $\Psi^{(2)}$ containing

the effect of buoyancy in the boundary layer is more significant than the correction due to the displacement effect on the outer flow for $n > \frac{2}{5}$. For the non-diffusive case, this occurred for $n > \frac{4}{5}$.

The above analysis can be shown to reduce to the non-diffusive case discussed in (I) by considering the limit of (32) and (37) as the Prandtl number becomes large. When the Prandtl number is large, the first-order temperature field h_1 decays exponentially to zero in a thermal boundary which is of order $P_0^{-\frac{1}{3}}$ times the scale of the velocity boundary layer. The forcing term on the right-hand side of (37*a*) then vanishes, and f_2 vanishes as well since it satisfies a homogeneous equation with homogeneous boundary conditions. Thus, noting that h_1' and h_2'' are zero outside a very thin thermal layer near the wall, the solution of (37*b*) is

$$h_2(\eta) = (\beta/\theta)\,(f_1(\eta) - \eta). \tag{39}$$

The expansion for the stream function must then take the form

$$\psi(x,z) = R_L^{-\frac{1}{2}}\,[x^{\frac{1}{2}} f_1(\eta) + R_L^{n-\frac{1}{2}} x(0) + R^{n-1} x^{\frac{3}{2}} f_3(\eta) + \ldots], \tag{40}$$

and f_3 is identical with the function noted as f_2 in I(§7, equations (61) and (62)). Consequently, the difficulty encountered there (see I, equation (63)) appears in the diffusive solutions also, for an extension of the preceding analysis ($P_0 \simeq O(1)$) to the next higher-order term in the boundary-layer expansion would result in a vorticity equation containing a non-zero forcing term at the edge of the boundary layer. This difficulty may be peculiar to the geometry of the problem, since, as shown in I, the boundary-layer solution is valid only for a plate of finite length.

5. Numerical results

Equations (32) and (37) were integrated numerically using Hamming's modified predictor-corrector method for the solution of general initial value problems (cf. Ralston & Wilf 1960, pp. 95–109). The integration was accomplished by transforming (32*a*) to an equivalent initial-value problem (cf. Rosenhead 1963, p. 223), solving for f_1, and then solving (32*b*), (37*a*), and (37*b*) successively in that order. A maximum error bound of 10^{-4} was imposed in the numerical approximation. If the absolute error exceeded the specified bound, the integration step-size was halved. Numerical solutions were obtained for a range of each of the three parameters Ru_L, P_0, and β/θ in order to determine their individual influence on the properties of the boundary layer.

A measure of the effect of stratification on the boundary layer is obtained by evaluating its influence on the shear and heat transfer at the plate surface. Using the previous results, the following expressions for the skin-friction and heat-transfer coefficients can be derived:

$$C_f = \frac{\tau_0}{\rho_0 U_0^2} = \frac{f_1''(0)}{R_{x_1}^{\frac{1}{2}}}\left[1 + x^{\frac{1}{2}} R_L^{n-\frac{1}{2}} \frac{f_2''(0)}{f_1''(0)}\right] \quad (0 \leqslant n < \tfrac{1}{2}), \tag{41}$$

and

$$C_h = \frac{q_0}{\rho_0 c_{p_0} U_0 (T_0 - T_w)} = \frac{h_1'(0)}{P_0 R_{x_1}^{\frac{1}{2}}}\left[1 + x^{\frac{1}{2}} R_L^{-\frac{1}{2}} \frac{q_2(0)}{h_1'(0)}\right] \quad (n = 0), \tag{42}$$

where R_{x_1} is the Reynolds number based on the dimensional length x_1 measured from the leading edge of the plate, and $q_2(0)$ is defined by the relation

$$q_2(0) = h_2'(0) + \beta/\theta. \tag{43}$$

The symbols τ_0 and q_0 denote the shear and heat flux, respectively, at the plate surface. Stratification and buoyancy have an effect only in the second-order terms. The second-order temperature field was evaluated only for the case $n = 0$, but the velocity field is computed for the range $0 \leqslant n < \frac{1}{2}$.

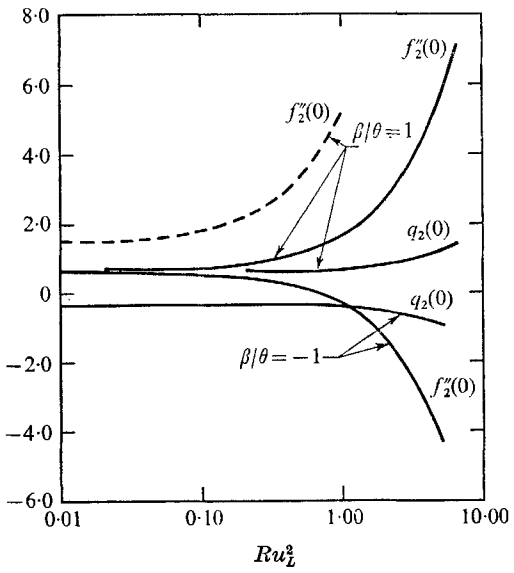

FIGURE 3

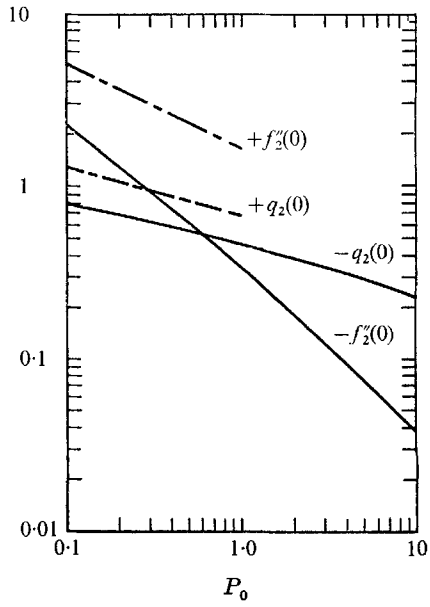

FIGURE 4

FIGURE 3. The variation of the second-order shear and heat transfer with the Russell number. —, $P_0 = 1{\cdot}0$; - - -, $P_0 = 0{\cdot}1$.

FIGURE 4. The variation of the second-order shear and heat transfer with the Prandtl number ($Ru_L = 1{\cdot}0$). —, $\beta/\theta = -1$; ———, $\beta/\theta = 1$.

The results show that the Russell number has a very significant effect on the structure of the boundary layer. Figure 3 exhibits the influence of Ru_L on the skin-friction and heat transfer for both a heated and cooled wall. The second-order contribution to the shear changes profoundly when the Russell number is of order unity or larger. When the boundary is heated relative to the external stream, the skin-friction increases as the Russell number increases and vice versa for a cooled boundary. Stratification then acts to prevent separation on heated boundaries and promotes separation, at least for large Russell numbers, on cooled boundaries.

Figure 4 portrays the influence of the Prandtl number on the boundary-layer properties for a fixed Russell number and wall to free-stream temperature ratio. The Prandtl numer has a very strong effect on the shear at the boundary. This is attributable to the fact that the thermal boundary-layer thickness and the first-

order temperature field depend strongly on the Prandtl number and, therefore, affect the second-order velocity field through the right-hand side of (37*a*).

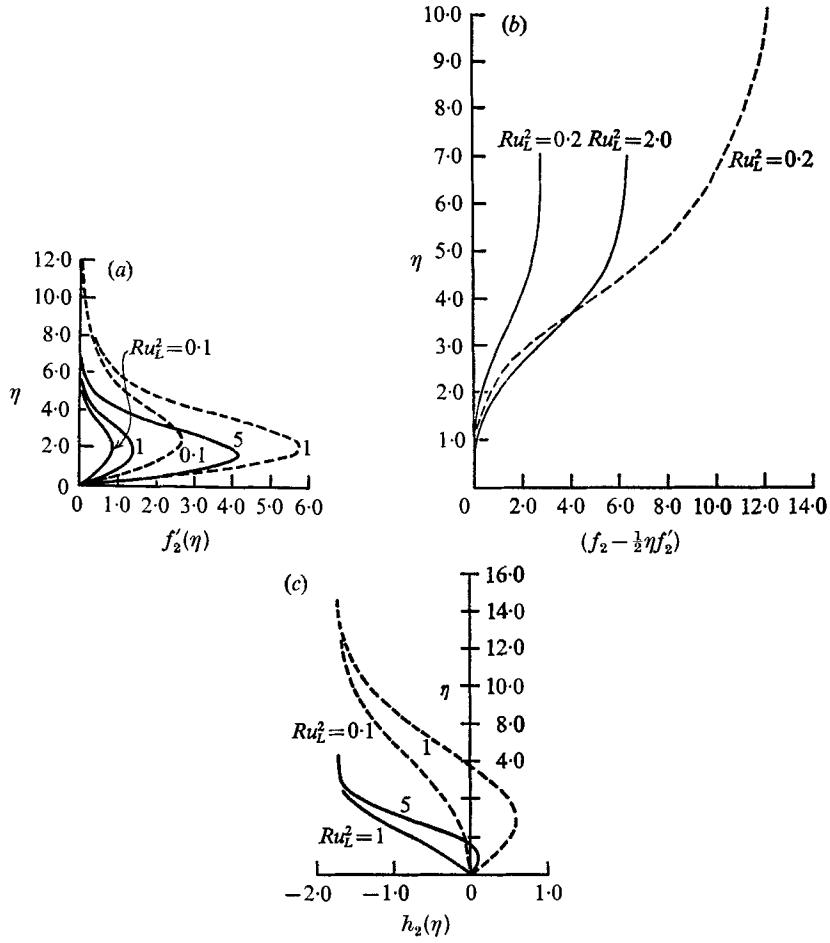

FIGURE 5. The effect of the Russell and Prandtl numbers on the boundary-layer profiles: (*a*) horizontal velocity, (*b*) vertical velocity, and (*c*) temperature. $\beta/\theta = 1$. —, $P_0 = 1{\cdot}0$; - - -, $P_0 = 0{\cdot}1$.

Representative second-order horizontal and vertical velocity profiles and temperature profiles are shown in figure 5. The total velocity and temperature in the boundary layer can be computed from the relations

$$u = f_1'\left[1 + x^{\frac{1}{2}}R_L^{n-\frac{1}{2}}\frac{f_2'}{f_1'}\right] \quad (0 \leqslant n < \tfrac{1}{2}), \tag{44}$$

$$w = -\tfrac{1}{2}R_{x_1}^{\frac{1}{2}}(f_1 - \eta f_1')\left[1 + 2x^{\frac{1}{2}}R_L^{n-\frac{1}{2}}\left(\frac{f_2 - \frac{1}{2}\eta f_2'}{f_1 - \eta f_1'}\right)\right] \quad (0 \leqslant n < \tfrac{1}{2}), \tag{45}$$

and

$$T = h_1\left[1 + x^{\frac{1}{2}}R_L^{-\frac{1}{2}}\frac{h_2}{h_1}\right] \quad (n = 0). \tag{46}$$

The figure clearly shows that buoyancy (Ru_L) and diffusion (P_0) have a strong influence on the velocity profile, especially for large Russell numbers and small

Prandtl numbers. Since the second-order contribution grows with distance from the leading edge, these effects may be quite pronounced near the trailing edge of the plate. Also, when the Russell number is large (n close to $\frac{1}{2}$), the mean velocity profile is significantly different from the Blasius profile. Stratification, therefore,

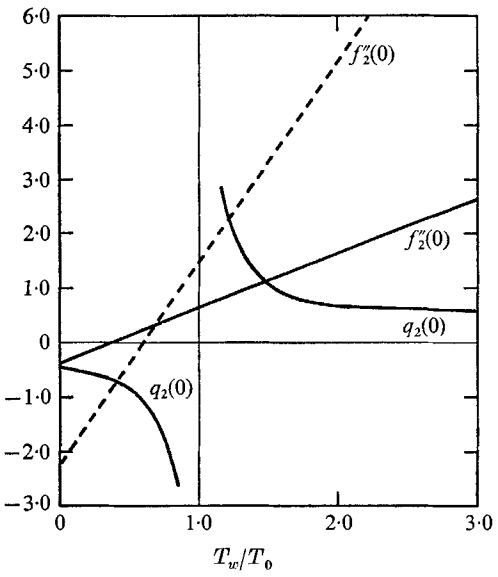

FIGURE 6

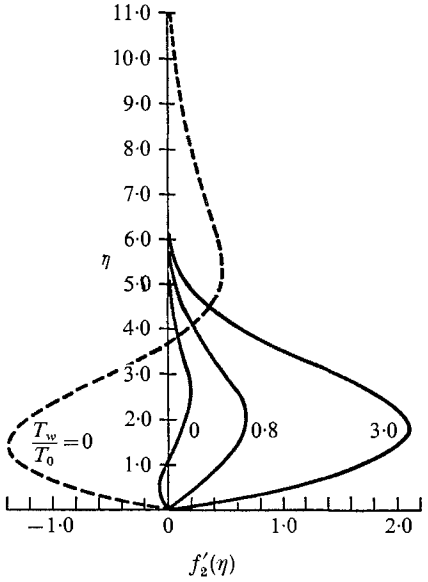

FIGURE 7 (*a*)

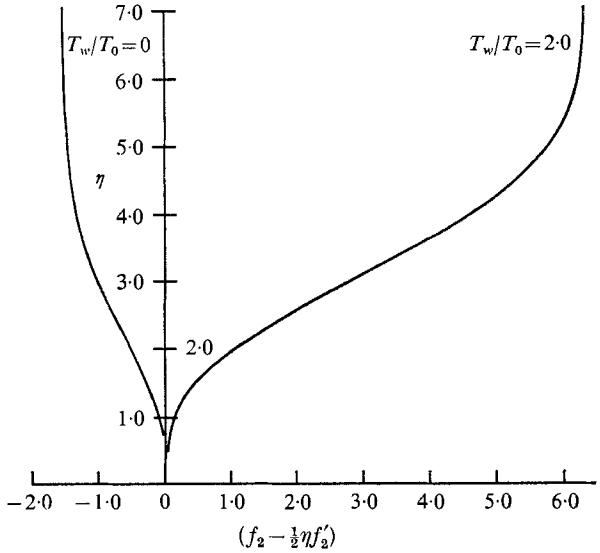

FIGURE 7 (*b*)

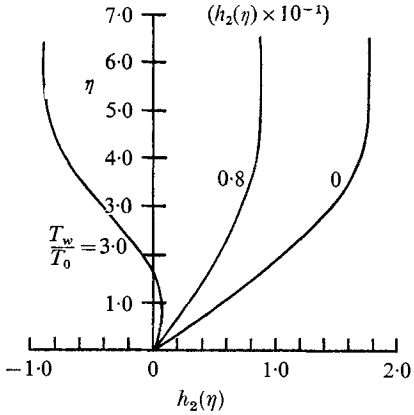

FIGURE 7 (*c*)

FIGURE 6. The second-order shear and heat transfer as a function of the wall-to-free-stream temperature ratio: ($Ru_L = 1·0$, $\beta = 1·0$). —, $P_0 = 1·0$; - - -, $P_0 = 0·1$.

FIGURE 7. The effect of the wall-to-free-stream temperature ratio on the boundary-layer profiles. (*a*) Horizontal velocity: $Ru_L = 1·0$; —, $P_0 = 1·0$; - - -, $P_0 = 0·1$. (*b*) Vertical velocity: $Ru_L^2 = 2·0$, $P_0 = 1·0$. (*c*) Temperature: $Ru_L = 1·0$, $P_0 = 1·0$.

can have an important effect on the stability of a boundary layer through its modification of the mean profile as well as through the effect of buoyancy on the velocity perturbations superimposed on the mean flow.

The wall to free-stream temperature ratio also plays a role in determining the characteristics of the stratified boundary layer. Its importance is depicted in figures 6 and 7 which contain results for a fixed stratification ($\beta_0 L = 1$) and fixed Russell number. The function $q_2(0)$ is singular at $T_w/T_0 = 1$ because the parameter β/θ in (37*b*, *c*) goes to infinity as T_w approaches T_0. This is a consequence of the temperature scaling expressed in (6). The shear is seen to increase rapidly as the wall is heated.

6. Summary

In summary, the combined effect of thermal stratification and buoyancy on a horizontal boundary layer is greatest when the wall is heated and the Prandtl number is small. The Prandtl number is particularly important since it determines the vertical scale (the thickness of the thermal boundary layer) over which buoyancy forces can act. Also, stratification can either enhance or impede separation depending on the relative temperature of the boundary and free-stream and the magnitude of the Froude number.

Diffusion has a very significant effect in that it serves to emphasize the importance of the buoyancy term by coupling the velocity and thermal fields. This is of primary importance when the Froude number is small (or large Russell number) which indicates that diffusion may considerably alter the structure of the upstream boundary layer studied by Martin & Long (1968) and Pao (1968), especially in the vicinity of the trailing edge of a plate of finite length. Furthermore, since the diffusion boundary layer always grows from the leading edge, a downstream momentum wake arising from the resultant density variation should exist even in the case when the viscous boundary layer grows in the upstream direction.

The author acknowledges the many helpful discussions with Professors R. E. Kelly and A. F. Charwat during the course of this investigation. The research was supported by the National Science Foundation under Grant GK-4213 and was performed as part of the author's doctoral dissertation at the School of Engineering and Applied Science, UCLA.

REFERENCES

KELLY, R. E. & REDEKOPP, L. G. 1970 The development of horizontal boundary layers in stratified flow. Part 1. Non-diffusive flow. *J. Fluid Mech.* **42**, 497.

MARTIN, S. & LONG, R. R. 1968 The slow motion of a flat plate in a viscous stratified fluid. *J. Fluid Mech.* **31**, 669–688.

PAO, Y. H. 1968 Laminar flow of a stably stratified fluid past a flat plate. *J. Fluid Mech.* **34**, 795–808.

RALSTON, A. & WILF, H. S. 1960 *Mathematical Methods for Digital Computers.* New York: Wiley.

ROSENHEAD, L. (Ed.) 1963 *Laminar Boundary Layers.* Oxford University Press.

SCHLICHTING, H. 1968 *Boundary Layer Theory.* New York: McGraw-Hill.